

## Room temperature ferromagnetism in cubic GaN epilayers implanted with Mn<sup>+</sup> ions

V. A. Chitta,<sup>a)</sup> J. A. H. Coaquira, J. R. L. Fernandez, C. A. Duarte, and J. R. Leite  
*Instituto de Física da Universidade de São Paulo, Caixa Postal 66318, 05315-970 São Paulo, SP, Brazil*

D. Schikora, D. J. As, and K. Lischka  
*Universität Paderborn, FB6 Physic, D-33095 Paderborn, Germany*

E. Abramof  
*Instituto Nacional de Pesquisas Espaciais (INPE-LAS), Caixa Postal 515,  
 12901-970 São José dos Campos, SP, Brazil*

(Received 8 June 2004; accepted 6 September 2004)

Mn ions were implanted in *p*-type cubic GaN at doses from 0.6 to  $2.4 \times 10^{16}$  cm<sup>-2</sup> at 200 keV energy. A 200-nm-thick epitaxial layer, grown by molecular beam epitaxy on GaAs(001) substrate, is used for the Mn implantation. The Mn implanted samples were subjected to an annealing at 950 °C for 1–5 min. The structural quality of the samples was investigated by high resolution x-ray diffraction and Raman spectroscopy. The annealing procedure leads to a significant increasing of the crystalline quality of the samples. Hysteresis loops were observed for all cubic GaMnN annealed samples and ferromagnetism was detected up to room temperature. © 2004 American Institute of Physics. [DOI: 10.1063/1.1812590]

Group-III nitrides semiconductors have attracted much interest due to their usefulness in short-wavelength optoelectronics and high voltage, high-temperature, and high-frequency electronic devices.<sup>1–4</sup> Especially, cubic (zinc blende) GaN has received much attention since the successful fabrication of light-emitting diodes based on structures built up using this material.<sup>5–10</sup> On the other hand, since the discovery of carrier induced ferromagnetism in InMnAs and GaMnAs, the interest in diluted magnetic semiconductors (DMS) has renewed. However, due to the low Curie temperature,  $T_C$ , presented by these compounds, new DMS materials should be developed to be used in practical applications. Theoretically, Dietl *et al.*<sup>11</sup> using the Zener model, in which the ferromagnetic interaction between the localized moments is considered to be mediated by holes, calculated the Curie temperature for different III–V and II–VI semiconductors containing 5% of Mn and a hole concentration of  $3.5 \times 10^{20}$  cm<sup>-3</sup>. In particular, they predicted a  $T_C$  above room temperature for GaMnN. Several experimental results on the magnetic properties of hexagonal (wurtzite) GaN-based DMS can be found in the literature.<sup>12–19</sup> Nevertheless, the results are not conclusive, since a paramagnetic as well as a ferromagnetic behavior has been observed, with a great variation of  $T_C$ . The very few experimental studies of cubic GaN-based DMS are restricted so far to the investigations of structural and electrical properties of GaMnN layers.<sup>20,21</sup> Recently, *p*-type conductivity in cubic GaMnN layers grown by molecular beam epitaxy on GaAs(001) substrates was observed.<sup>21</sup> Also recently, in a theoretical work, ferromagnetism in the metallic phase of cubic GaMnN layers was studied by Monte Carlo simulations and Curie transition temperatures high above room temperature were predicted.<sup>22</sup>

In this letter we report on the investigation of the magnetic properties of cubic GaN implanted with Mn ions. In contrast with the stable hexagonal phase, the cubic samples

are free of spontaneous polarization and strain-induced piezoelectric field, which can provide much longer spin relaxation times. Moreover, for cubic GaN we expect a Curie temperature 6% higher than for the wurtzite structure.<sup>11</sup> The cubic GaN sample was grown by plasma-assisted molecular beam epitaxy, using a Riber-32 system, equipped with elemental sources of Ga and As, and an Oxford Applied Research CARS 25 rf-activated plasma source. The 200-nm-thick layer was grown on a GaAs(001) substrate at a temperature of 720 °C. Details of the growth procedure were reported in Ref. 23. Four pieces of the same sample were implanted with four different doses of Mn ions as shown in Table I. The energy and temperature of implantation were kept constant at 200 keV and 350 °C, respectively. The implanted layer is estimated to be centered at approximately 110 nm from the surface and the implanted doses to correspond roughly to Mn concentrations varying from 1% to 3%. After implantation the samples were annealed up to 5 min at 950 °C under flowing nitrogen.

The structural quality of the samples was inspected by high resolution x-ray diffraction and Raman spectroscopy. The x-ray spectra show that after implantation and annealing the samples conserved their cubic structure with no appearance of hexagonal inclusions. This was also confirmed by the Raman measurements as can be seen in Fig. 1 where the spectra, obtained at 10 K, for the samples before implantation (460—thin solid line), 460B just after implantation (dot-

TABLE I. Implantation doses ( $d$ ), annealing time at 950 °C ( $t$ ), and estimated Mn concentration ( $x$ ).

Sample	$d$ (cm <sup>-2</sup> )	$t$ (min)	$x$ (%)
460	...	...	0
460A	$6.0 \times 10^{15}$	1	0.7
460B	$1.2 \times 10^{16}$	1	1.4
460C	$1.8 \times 10^{16}$	1	2.1
460D	$2.4 \times 10^{16}$	5	2.8

<sup>a)</sup>Electronic mail: vchitta@macbeth.if.usp.br

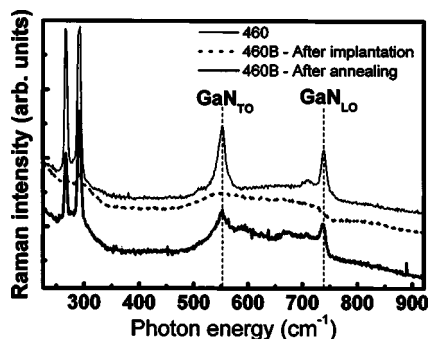


FIG. 1. Raman spectra of sample 460 (thin solid line) and 460B just after implantation (dotted line) and after annealing of 1 min at 950 °C (thick solid line). The vertical-dotted lines denote the transverse-optical (TO) and longitudinal-optical (LO) cubic GaN phonon frequencies.

ted line), and 460B after 1 min of annealing (thick solid line) are depicted. The Raman spectrum of the sample before implantation shows the characteristic transverse-optical (TO) and longitudinal-optical (LO) phonon frequencies of cubic GaN at 555 and 741 cm<sup>-1</sup>, respectively.<sup>24</sup> As can be observed, just after implantation, the sample shows a curve characteristic of an almost amorphous material, with all the characteristic peaks being smeared out, including the peaks related to GaAs, indicating that the substrate has also been disturbed by the implantation. After 1 min of annealing the crystalline quality has been partially recovered and, increasing the annealing time, this improves. In all the spectra no traces of hexagonal phase can be observed.

The electrical characteristics of the samples were measured at room temperature. The nonimplanted sample (460 in Table I) displays an intrinsic hole concentration of  $3.7 \times 10^{17} \text{ cm}^{-3}$ . A slight improvement in the hole concentration is observed after implantation and annealing. This could be attributed to the introduction of the Mn ions, but, as it has been reported,<sup>25,26</sup> the energy level induced by Mn in GaN is located deep in the gap, and thus would be an ineffective acceptor dopant. On the other hand, since stoichiometry effects, crystal defects, unintentional impurities, and conduction through the substrate may control the final conductivity, the annealing rather than the introduction of Mn could be responsible for this improvement.

Magnetization measurements of the Mn implanted cubic GaN, performed with a superconducting quantum interference device, showed them to be ferromagnetic below room temperature. In Fig. 2, we show the magnetic moment as a function magnetic field, measured at 10 K, for the annealed samples 460B, 460C, and 460D. We observe hysteresis loop for all of our implanted samples and, as the implantation

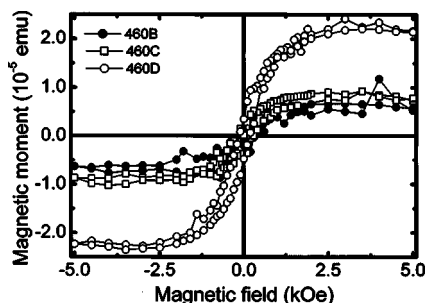


FIG. 2. Magnetic moment as a function of magnetic field at 10 K for samples 460B, 460C, and 460D.

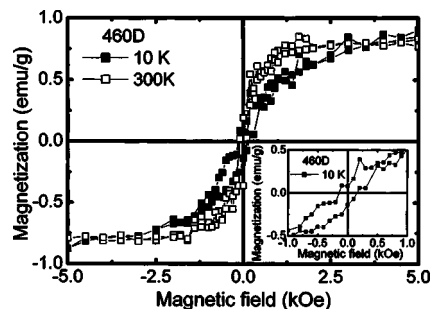


FIG. 3. Magnetization as a function of magnetic field at 10 and 300 K for sample 460D. The inset shows the low field region magnetization, measured at 10 K, where hysteresis can be observed.

doses increase, the magnetic moment at saturation increases too. The reference sample (nonimplanted) shows only the characteristic diamagnetic response, i.e., no hysteresis loop is observed for this sample.

The magnetization versus magnetic field curves for the highly Mn-implanted GaN epilayer, measured at 10 and 300 K, are presented in Fig. 3. At 300 K the magnetization increases steeply at low fields, and saturates at approximately 2.5 kOe. The increase in magnetization at 10 K is less accentuated, possibly due to a paramagnetic contribution. The curves show hysteresis for both temperatures, with coercive fields of 150 and 100 Oe for 10 and 300 K, respectively. This hysteresis at low field, for the magnetization measured at 10 K, is shown in the inset of Fig. 3. A remanent magnetization of about 0.1–0.2 emu/g can also be observed. From the saturation value we can obtain the number of active Mn atoms,  $N_{\text{Mn}} = M_S / g \mu_B S$ , where  $M_S$  is the magnetization at saturation,  $g=2$  is the  $g$  factor of Mn,  $\mu_B$  is the Bohr magneton, and  $S=5/2$  if we consider Mn<sup>2+</sup>. Taking  $M_S \approx 0.8 \text{ emu/g}$  we obtain  $N_{\text{Mn}} = 8.9 \times 10^{19} \text{ cm}^{-3}$ , which correspond to an effective Mn concentration of only 0.2%.

The temperature-dependent magnetization for the sample implanted with  $2.4 \times 10^{16} \text{ cm}^{-2}$  Mn ions is presented in Fig. 4. The shape of the curves is very similar to those obtained from implanted hexagonal GaN,<sup>16</sup> and may indicate the presence of a paramagnetic phase at low temperatures, as can also be inferred from the hysteresis loop at 10 K. We can attribute the ferromagnetic behavior observed in our samples to the presence of Mn in the GaN layer. Even with the GaAs substrate being disturbed by the Mn implantation, as shown by the Raman spectra, we can expect a negligible contribution from the substrate to the magnetic characteristic of our samples. With the doses and energy used for the implantation, we can expect a very small concentration of Mn at the substrate, near the interface with the GaN layer. As shown by

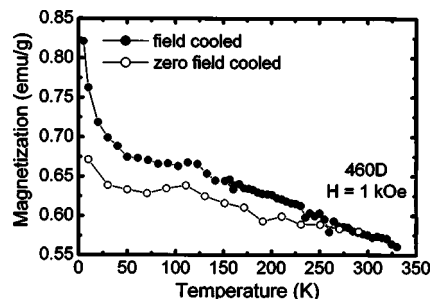


FIG. 4. Field-cooled (FC) and zero field-cooled (ZFC) magnetization as a function of temperature for sample 460D.

Song *et al.*,<sup>27</sup> the magnetization measured in GaAs implanted with  $7.5 \times 10^{17} \text{ cm}^{-2}$  Mn ions, which is 30 times larger than the highest dose we have used, is two orders of magnitude smaller than the magnetization we measured in our samples.

In conclusion, we show that cubic GaN films implanted with Mn ions clearly exhibit ferromagnetism at room temperature. At this point we are unable to clearly establish the origin of ferromagnetism in our samples. It is certainly reasonable to say that the origin of ferromagnetism in diluted magnetic semiconductors based on GaN is still not totally understood. However, ferromagnetism has been observed in samples with hexagonal structure that have very low hole concentrations, in insulating material, even in *n*-type material. The expected fact that GaMnN with cubic structure also exhibits interesting ferromagnetic properties is confirmed here.

This work was supported by *Fundação de Amparo à Pesquisa do Estado de São Paulo (FAPESP)*, *Conselho Nacional de Desenvolvimento Científico e Tecnológico (CNPq)* and *Deutsche Forschungsgemeinschaft (DFG)*. The authors are thankful to Professor I. Baumvol and Professor F. Zawislak for the ion implantations carried out at the Physics Institut, UFRGS.

<sup>1</sup>S. Strite and H. Marcoç, *J. Vac. Sci. Technol. B* **10**, 1237 (1992).

<sup>2</sup>S. Nakamura and G. Fasol, *The Blue Laser Diode* (Springer, Berlin, 1997).

<sup>3</sup>J. Orton and C. Foxon, *Rep. Prog. Phys.* **61**, 1 (1998).

<sup>4</sup>P. Kung and M. Razeghi, *Opto-Electron. Rev.* **8**, 201 (2000).

<sup>5</sup>S. F. Chichibu, A. C. Abare, M. P. Mack, M. S. Minsky, T. Deguchi, D. Cohen, P. Kozodoy, S. B. Fleischer, S. Keller, J. S. Speck, J. E. Bowers, E. Hu, U. K. Mishra, L. A. Coldre, S. P. Den Baars, K. Wada, T. Sota, and S. Nakamura, *Mater. Sci. Eng., B* **59**, 298 (1999).

<sup>6</sup>L.M. R. Scolfaro, *Phys. Status Solidi A* **190**, 15 (2002).

<sup>7</sup>H. Yang, L. X. Zheng, J. B. Li, X. J. Wang, D. P. Xu, Y. T. Wang, X. W. Hu, and P. D. Han, *Appl. Phys. Lett.* **74**, 2498 (1999).

<sup>8</sup>D. J. As, A. Richter, J. Busch, M. Lübbbers, J. Minikes, and K. Lischka, *Appl. Phys. Lett.* **76**, 13 (2000).

<sup>9</sup>H. Gomez-Cuatzin, J. Tardy, P. Rojo-Romeo, A. Philippe, C. Bru-Chevalier, A. Souifi, G. Guillot, E. Martinez-Guerrero, G. Feuillet, B. Daudin, P. Aboughé-Nzé, and Y. Monteil, *Phys. Status Solidi A* **176**, 131

(1999).

<sup>10</sup>Y. Taniyasu, K. Suzuki, D. H. Lim, A. W. Jia, M. Shimotomai, Y. Kato, M. Kobayashi, A. Yoshikawa, and K. Takahashi, *Phys. Status Solidi A* **180**, 241 (2000).

<sup>11</sup>T. Dietl, H. Ohno, F. Matsukura, J. Cibert, and D. Ferrand, *Science* **287**, 1019 (2000).

<sup>12</sup>M. Zajac, R. Doradzinski, J. Gosk, J. Szczytko, M. Lefeld-Sosnowska, M. Kaminska, A. Towardowski, M. Palczewska, E. Grzanka, and W. Gebicki, *Appl. Phys. Lett.* **78**, 1276 (2001).

<sup>13</sup>M. Zajac, J. Gosk, M. Kaminska, A. Towardowski, T. Szyszko, and S. Podsiadlo, *Appl. Phys. Lett.* **79**, 2432 (2001).

<sup>14</sup>M. L. Reed, M. K. Ritums, H. H. Stadelmaier, M. J. Reed, C. A. Parker, S. M. Bedair, and N. A. El-Masry, *Mater. Lett.* **51**, 500 (2001).

<sup>15</sup>M. L. Reed, N. A. El-Masry, H. H. Stadelmaier, M. E. Ritums, N. J. Reed, C. A. Parker, J. C. Roberts, and S. M. Bedair, *Appl. Phys. Lett.* **79**, 3473 (2001).

<sup>16</sup>N. A. Theodoropoulou, A. F. Hebard, M. E. Overberg, C. R. Abernathy, S. J. Pearton, S. N. G. Chu, and R. G. Wilson, *Appl. Phys. Lett.* **78**, 3475 (2001).

<sup>17</sup>S. Sonoda, S. Shimizu, T. Sasaki, Y. Yamamoto, and H. Hori, *J. Cryst. Growth* **237**, 1358 (2002).

<sup>18</sup>G. T. Thaler, M. E. Overberg, B. Gila, R. Frazier, C. R. Abernathy, S. J. Pearton, J. S. Lee, S. Y. Lee, Y. D. Park, Z. G. Khim, J. Kim, and F. Ren, *Appl. Phys. Lett.* **80**, 3964 (2002).

<sup>19</sup>S. J. Pearton, C. R. Abernathy, M. E. Overberg, G. T. Thaler, D. P. Norton, N. Theodoropoulou, A. F. Hebard, Y. D. Park, F. Ren, J. Kim, and L. A. Boatner, *J. Appl. Phys.* **93**, 1 (2003).

<sup>20</sup>Y. Cui, V. K. Lazarov, M. M. Goetz, H. Liu, D. P. Robertson, M. Gajdardziska-Josifovska, and L. Li, *Appl. Phys. Lett.* **82**, 4666 (2003).

<sup>21</sup>S. V. Novikov, K. W. Edmonds, A. D. Giddings, K. Y. Wang, C. R. Staddon, R. P. Campion, B. L. Gallagher, and C. T. Foxon, *Semicond. Sci. Technol.* **19**, L13 (2004).

<sup>22</sup>M. A. Boselli, I. C. da Cunha Lima, J. R. Leite, A. Troper, and A. Ghazali, *Appl. Phys. Lett.* **84**, 1138 (2004).

<sup>23</sup>D. Schikora, M. Hankeln, D. J. As, K. Lischka, T. Litz, A. Waag, T. Buhrow, and F. Henneberger, *Phys. Rev. B* **54**, R8381 (1996).

<sup>24</sup>A. Tabata, R. Enderlein, J. R. Leite, S. W. da Silva, J. C. Galzerani, D. Schikora, M. Kloidt, and K. Lischka, *J. Appl. Phys.* **79**, 4137 (1996).

<sup>25</sup>R. Y. Korotkov, J. M. Gregie, and B. W. Wessels, *Appl. Phys. Lett.* **80**, 1731 (2002).

<sup>26</sup>T. Graf, M. Gjukic, M. S. Brandt, M. Stutzmann, and O. Ambacher, *Appl. Phys. Lett.* **81**, 5159 (2002).

<sup>27</sup>S. -L. Song, N. -F. Chen, J. -P. Zhou, Z. -G. Yin, Y. -L. Li, S. -Y. Yang, and Z. -K. Liu, *J. Cryst. Growth* **264**, 31 (2004).